Acta Neuropathol
DOI 10.1007/s00401-012-1020-6

ORIGINAL PAPER

Transportin 1 accumulates specifically with FET proteins but no other transportin cargos in FTLD-FUS and is absent in FUS inclusions in ALS with *FUS* mutations

Manuela Neumann · Chiara F. Valori · Olaf Ansorge · Hans A. Kretzschmar · David G. Munoz · Hirofumi Kusaka · Osamu Yokota · Kenji Ishihara · Lee-Cyn Ang · Juan M. Bilbao · Ian R. A. Mackenzie

Received: 22 May 2012 / Accepted: 16 July 2012

Abstract Accumulation of the DNA/RNA binding protein fused in sarcoma (FUS) as inclusions in neurons and glia is the pathological hallmark of amyotrophic lateral sclerosis patients with mutations in *FUS* (ALS-*FUS*) as well as in several subtypes of frontotemporal lobar degeneration (FTLD-FUS), which are not associated with *FUS* mutations. Despite some overlap in the phenotype and neuropathology of FTLD-FUS and ALS-*FUS*, significant differences of potential pathomechanistic relevance were recently identified in the protein composition of inclusions in these conditions. While ALS-*FUS* showed only accumulation of FUS, inclusions in FTLD-FUS revealed co-accumulation of all members of the FET protein family, that include FUS, Ewing's sarcoma (EWS) and TATA-binding protein-associated factor 15 (TAF15) suggesting a more complex disturbance of transportin-mediated nuclear import of proteins in FTLD-FUS compared to ALS-*FUS*. To gain more insight into the mechanisms of inclusion body formation, we investigated the role of Transportin 1 (Trn1) as well as 13 additional cargo proteins of Transportin in the spectrum of FUS-opathies by immunohistochemistry and biochemically. FUS-positive inclusions in six ALS-*FUS* cases including four different mutations did not label for Trn1. In sharp contrast, the FET-positive pathology in all

Electronic supplementary material The online version of this article (doi:10.1007/s00401-012-1020-6) contains supplementary material, which is available to authorized users.

M. Neumann · C. F. Valori
Institute of Neuropathology, University Hospital Zurich, Zurich, Switzerland

M. Neumann (✉)
Department of Neuropathology, University of Tübingen, Calwerstr. 3, 72076 Tübingen, Germany
e-mail: Manuela.Neumann@med.uni-tuebingen.de

M. Neumann
DZNE, German Center for Neurodegenerative Diseases, Tübingen, Germany

O. Ansorge
Department of Neuropathology, John Radcliffe Hospital, Oxford, UK

H. A. Kretzschmar
Center for Neuropathology and Prion Research, Ludwig-Maximilians-University, Munich, Germany

D. G. Munoz
Department of Laboratory Medicine and Pathobiology, Li Ka Shing Knowledge Institute, St. Michael's Hospital, University of Toronto, Toronto, Canada

H. Kusaka
Department of Neurology, Kansai Medical University, Osaka, Japan

O. Yokota
Department of Neuropsychiatry, Okayama University Graduate School of Medicine, Dentistry and Pharmaceutical Sciences, Okayama, Japan

K. Ishihara
Department of Neurology, Showa University School of Medicine, Tokyo, Japan

L.-C. Ang
Department of Pathology, London Health Sciences Centre, London, ON, Canada

J. M. Bilbao
Department of Pathology, Sunnybrook Health Sciences Centre, Toronto, ON, Canada

I. R. A. Mackenzie
Department of Pathology, Vancouver General Hospital, University of British Columbia, Vancouver, Canada

Published online: 28 July 2012

FTLD-FUS subtypes was also strongly labeled for Trn1 and often associated with a reduction in the normal nuclear staining of Trn1 in inclusion bearing cells, while no biochemical changes of Trn1 were detectable in FTLD-FUS. Notably, despite the dramatic changes in the subcellular distribution of Trn1 in FTLD-FUS, alterations of its cargo proteins were restricted to FET proteins and no changes in the normal physiological staining of 13 additional Trn1 targets, such as hnRNPA1, PAPBN1 and Sam68, were observed in FTLD-FUS. These data imply a specific dysfunction in the interaction between Trn1 and FET proteins in the inclusion body formation in FTLD-FUS. Moreover, the absence of Trn1 in ALS-*FUS* provides further evidence that ALS-*FUS* and FTLD-FUS have different underlying pathomechanisms.

Keywords Transportin · FUS · TAF15 · EWS · Amyotrophic lateral sclerosis · Frontotemporal dementia

Introduction

Amyotrophic lateral sclerosis (ALS) and frontotemporal lobar degeneration (FTLD) are clinically, genetically and neuropathologically heterogeneous groups of neurodegenerative diseases. The neuropathology is characterized by the abnormal intracellular accumulation of specific proteins with the accumulation of the fused in sarcoma protein (FUS, also known as translocated in liposarcoma, TLS) being the characteristic lesion in ~3 % of ALS cases and ~10 % of FTLD cases, subsumed as FTLD-FUS [20].

FUS is a multifunctional DNA/RNA binding protein and belongs to the FET family of proteins that also includes Ewing's sarcoma (EWS) protein, TATA-binding protein-associated factor 15 (TAF15) and the drosophila orthologue Cabeza [14, 17]. The FET proteins are predominantly nuclear, ubiquitously expressed, highly conserved proteins with predicted roles in RNA transcription, processing, transport, microRNA processing and DNA repair [14, 17, 34]. All of the FET proteins are shuttling proteins [12, 39, 40] and their nuclear import is mediated by a non-classical nuclear localization signal, called PY-NLS, recognized by the nuclear import protein Transportin 1 (Trn1) [7, 18].

ALS cases with FUS pathology are almost always associated with a mutation in the *FUS* gene (ALS-*FUS*). Mutations in the gene *FUS* were first identified in 2009 as the cause of familial ALS type 6 [15, 37] and then rapidly confirmed in large ALS cohorts accounting for ~3 % of familial and <1 % of sporadic ALS [20]. The neuropathology of ALS-*FUS* is characterized by abnormal cytoplasmic inclusions in neurons and glia that are immunoreactive for FUS [3, 9, 10, 15, 29, 37]. Significant pathological heterogeneity with respect to morphological and regional distribution of FUS pathology has been described in ALS-*FUS* allowing delineation of two distinct patterns correlating with disease severity and specific mutations [23]. The majority of *FUS* mutations cluster in the C terminus of the protein which includes its PY-NLS. They have been shown to disrupt the PY-NLS motif leading to impaired Trn1-mediated nuclear import of FUS and subsequent increase of cytoplasmic FUS levels [7, 11, 13]. Notably, the level of nuclear import impairment that results from specific *FUS* mutations in cultured cells directly correlates with the clinical phenotype and the neuropathological patterns observed in ALS-*FUS*, thereby strongly suggesting that altered nuclear import of FUS is a key event in the pathogenesis of ALS-*FUS*.

FTLD-FUS includes three distinct clinico-pathological entities; atypical FTLD-U (aFTLD-U), basophilic inclusion body disease (BIBD) and neuronal intermediate filament inclusion disease (NIFID) [19, 24–26]. FTLD-FUS is mostly associated with sporadic early onset of behavioral variant of frontotemporal dementia with the exception of single cases with positive family history [16, 25, 26, 31, 32, 36]. While possibly other genetic factors might be involved in FTLD-FUS, in contrast to pure ALS with FUS pathology which is usually associated with *FUS* mutations, no genetic abnormalities of *FUS* have been identified in FTLD-FUS, and the mechanisms underlying inclusion body formation in FTLD-FUS remain unknown.

Although there is some clinical and pathological overlap between ALS-*FUS* and FTLD-FUS, the presence of significant differences in the genetics, phenotypes and the morphological patterns of FUS pathology [21] raised the question as to whether these conditions represent closely related conditions with a shared pathomechanism or whether the pathogenic pathways triggered by *FUS* mutations may be different from those involved in FTLD-FUS. Indeed, the analysis of the FUS homologues TAF15 and EWS has recently identified striking differences in the protein composition of inclusions in these conditions, with co-accumulation of all FET proteins in FTLD-FUS and restricted accumulation of only FUS in ALS-*FUS* [27]. These data provided strong evidence for different pathological processes underlying inclusion body formation and cell death between ALS-*FUS* and FTLD-FUS, with ALS-*FUS* being restricted to dysfunction of FUS, while FTLD-FUS seems to be associated with a broader and more complex dysregulation of Trn1-mediated nuclear import affecting all FET proteins and perhaps other Trn1 cargos.

In the present study, we extend our immunohistochemical analysis of the protein composition of inclusion bodies in the spectrum of FUS-opathies to Trn1 and 13 additional known Trn1 cargo proteins with a similar PY-NLS motif as FET proteins.

Methods

Case selection

The FUS-opathy cases included aFTLD-U ($n = 17$), BIBD ($n = 8$), NIFID ($n = 4$) and six ALS cases with four different *FUS* mutations. Most of these cases have been described in detail in previous studies [21, 23–27] and brief clinical and demographic features are summarized in Supplementary Table 1.

The original set of neurological control cases included FTLD-TDP ($n = 6$; two with subtype A (one with *GRN* mutation), two with subtype B (one with *C9ORF72* mutation) and two with subtype C [22]), FTLD-tau ($n = 6$; two Pick's disease, two corticobasal degeneration, and two progressive supranuclear palsy), FTLD with *CHMP2B* mutations ($n = 2$), FTLD-ni ($n = 3$), sporadic ALS with TDP pathology ($n = 2$), familial ALS with *SOD1* mutations ($n = 2$), Alzheimer's disease ($n = 2$), dementia with Lewy bodies ($n = 2$), Parkinson's disease ($n = 2$), multiple system atrophy ($n = 2$), Huntington's disease ($n = 2$), spinocerebellar ataxia ($n = 3$; one SCA-1 and two SCA-3) and neuronal intranuclear inclusion body disease ($n = 1$). When it was found that rare classical Lewy bodies in the substantia nigra of the cases of Parkinson's disease showed some Trn1 immunoreactivity, the following additional controls were added: sections of midbrain from six additional cases of Parkinson's disease, sections of hippocampus from two additional cases of dementia with Lewy bodies (to check if immunoreactivity was restricted to Lewy bodies in the substantia nigra) and sections of midbrain from three additional cases of PSP (to check if immunoreactivity was generalized to all types of cytoplasmic inclusions in nigral neurons). Normal control tissue ($n = 4$) was from elderly patients with no history of neurological disease.

Staining protocols for the 13 antibodies against other PY-NLS proteins (Table 3) were established using a tissue microarray including biopsy material from a glioblastoma and a brain metastasis of a colon carcinoma as well as postmortem tissue from the dentate granule cell layer and temporal cortex of three controls with no history of neurological disease.

Antibodies

A mouse monoclonal antibody was used for Trn1 immunohistochemistry (IHC) (clone 45, Abcam, 1:200). All FUS-opathy cases were stained for FUS (using either the polyclonal anti-FUS HPA008784, Sigma-Aldrich, 1:2,000 or the monoclonal anti-FUS, ProteintechGroup, 1:1,000), TAF15 using the polyclonal anti-TAF15 IHC-00094-1 (Bethyl Laboratories, 1:200), and EWS (using the monoclonal anti-EWS clone G5, Santa Cruz, 1:200, or the polyclonal anti-EWS IHC-00086, Bethyl Laboratories, 1:200). The list of antibodies against 13 other Trn1 cargo proteins with a PY-NLS investigated in this study is provided in Table 3.

Immunohistochemistry and double-label immunofluorescence

Trn1 IHC was performed on 5-μm thick sections of formalin-fixed paraffin-embedded tissue for all FUS-opathy and control cases on selected neuroanatomical regions known to have robust pathology using the Ventana BenchMark XT automated staining system (Ventana, Tuscon, AZ) following microwave antigen retrieval and developed with aminoethylcarbizole (AEC) or using the NovoLink™ Polymer Detection Kit and developed with DAB. Staining with antibodies against other PY-NLS

Table 1 Summary of Trn1 and FET protein immunoreactivity in the spectrum of FUS-opathies

Diagnosis	Number of cases (*n*)	Immunohistochemical profile of inclusions			
		Trn1	FUS	TAF15	EWS
FTLD-FUS					
aFTLD-U	17	pos	pos	pos	pos
BIBD	8	pos	pos	pos	pos
NIFID	4	pos	pos	pos	pos
ALS-*FUS*					
p.R521C	2	neg	pos	neg	neg
p.P525L	2	neg	pos	neg	neg
p.R514S/E516V	1	neg	pos	neg	neg
p.Q519lfsX9	1	neg	pos	neg	neg

aFTLD-U atypical frontotemporal lobar degeneration with ubiquitinated inclusions, *ALS-FUS* amyotrophic lateral sclerosis with *FUS* mutation, *BIBD* basophilic inclusion body disease, *NIFID* neuronal intermediate filament inclusion disease, *pos* positive, *neg* negative

Table 2 Immunoreactivity for Trn1 in other neurodegenerative diseases

Diagnosis	Regions examined	Trn1 immunoreactivity in signature lesions
AD	Frontal cortex, hippocampus	0/2
FTLD-TDP	Frontal cortex, hippocampus	0/6
FTLD with *CHMP2B*	Hippocampus	0/2
FTLD-tau (PSP)	Cerebellum, basal ganglia, midbrain	0/5[a]
FTLD-tau (CBD)	Basal ganglia	0/2
FTLD-tau (PiD)	Hippocampus	0/2
FTLD-ni	Hippocampus	0/3
ALS-TDP	Spinal cord	0/3
ALS with *SOD1*	Spinal cord	0/2
MSA	Pons, midbrain	0/2[b]
DLB	Hippocampus	0/4
PD	Midbrain	7/8[c]
SCA	Pons	0/3
HD	Basal ganglia	0/2
NIIBD	Hippocampus	0/1

AD Alzheimer's disease, *ALS-SOD1* amyotrophic lateral sclerosis with mutations in *SOD1* gene, *ALS-TDP* amyotrophic lateral sclerosis with TDP-43 pathology, *CBD* corticobasal degeneration, *DLB* dementia with Lewy bodies, *FTLD with CHMP2B* frontotemporal lobar degeneration with mutations in *CHMP2B* gene, *FTLD-ni* frontotemporal lobar degeneration with no inclusions, *FTLD-tau* frontotemporal lobar degeneration with tau pathology, *FTLD-TDP* frontotemporal lobar degeneration with TDP-43 pathology, *HD* Huntington's disease, *MSA* multiple system atrophy, *NIIBD* neuronal intranuclear inclusion body disease, *PD* Parkinson's disease, *PiD* Pick's disease, *PSP* progressive supranuclear palsy, *SCA* spinocerebellar ataxia

[a] Trn1 staining of coarse cytoplasmic granules in substantia nigra neurons, but no labeling of neurofibrillary tangles

[b] Trn1 staining of neuromelanin in substantia nigra neurons, but no labeling of glial cytoplasmic inclusions

[c] In addition to weak labeling of a small number (~2–14 %) of Lewy bodies in the substantia nigra in seven cases, all cases showed labeling of coarse cytoplasmic granules in substantia nigra neurons

proteins was performed on selected cases with severe FUS pathology (BIBD $n = 1$, aFTLD-U $n = 4$).

Incubation with primary antibodies was 32 min using the automated staining system or 1 h for non-automated staining procedure.

Double-label immunofluorescence (IF) was performed on selected cases for FUS, TAF15, EWS and Trn1 or FUS and other Trn1 substrates (Table 3). The secondary antibodies were Alexa Fluor 594 and Alexa Fluor 488-conjugated anti-mouse and anti-rabbit IgG (Invitrogen, 1:500). 4′-6-Diamidino-2-phenylindol (DAPI) was used for nuclear counterstaining. IF images were obtained by wide-field fluorescence microscopy (BX61 Olympus with digital camera F-view, Olympus).

Biochemical analysis

Fresh-frozen postmortem frontal grey matter from aFTLD-U ($n = 5$), BIBD ($n = 1$), NIFID ($n = 1$), FTLD with TDP-43 pathology ($n = 5$), and normal controls ($n = 4$) was used for the sequential extraction of proteins with buffers of increasing stringency, using an established protocol [25, 27]. Briefly, gray matter was extracted at 2 ml/g (v/w) by repeated homogenization and centrifugation steps (120,000×*g*, 30 min, 4 °C) with high-salt buffer (50 mM Tris–HCl, 750 mM NaCl, 10 mM NaF, 5 mM EDTA, pH 7.4), 1 % Triton-X 100 in HS buffer, radioimmunoprecipitation assay buffer [50 mM Tris–HCl, 150 mM NaCl, 5 mM EDTA, 1 % NP-40, 0.5 % sodium deoxycholate, 0.1 % sodium dodecyl sulfate (SDS)] and 2 % SDS buffer. To prevent carry over, each extraction step was performed twice. Only supernatants from the first extraction steps were analyzed while supernatants from the second wash steps were discarded. The 2 %-SDS insoluble pellet was extracted in 70 % formic acid at 0.5 ml/g (v/w), evaporated in a SpeedVac system and the dried pellet was resuspended in sample buffer and the pH was adjusted with NaOH. Protease inhibitors were added to all buffers prior to use. For immunoblot analysis, equal volumes of fractions from different samples (10 µl of high-salt and TX, 20 µl of RIPA and SDS, 25 µl of formic acid) were resolved by 7.5 % SDS-polyacrylamide gel electrophoresis and transferred to polyvinylidene difluoride membranes (Millipore, Billerica, MA, USA). Following transfer, membranes were blocked with Tris buffered saline containing 3 % powdered milk and probed with the mouse monoclonal anti-Trn1 antibody (clone 45, Abcam, 1:500) or polyclonal anti-FUS antibody (300-302A, Bethyl Laboratories, 1:10,000). Primary antibodies were detected with horseradish peroxidase-conjugated anti-rabbit or anti-mouse IgG (Jackson ImmunoResearch Europe, UK), signals were visualized by a chemiluminescent reaction (Millipore) and the Chemiluminescence Imager Stella 3200 (Raytest, Switzerland).

Results

Trn1 co-aggregates with FET proteins in all FTLD-FUS subtypes

Although there was some variation among cases and anatomical regions, the normal physiological staining pattern for Trn1 usually consisted of moderate to strong

Table 3 Trn1 cargo proteins with PY-NLS investigated in FTLD-FUS

Protein name	Antibody			Physiological staining pattern	Inclusions in FTLD-FUS
	Company	Dilution	Type		
FUS	ProteinTech Group (60160-1-Ig)	1:1,000	MM	nucl	pos
	Sigma (HPA008784)	1:2,000	RP	nucl	pos
TAF15	Bethyl Laboratories (IHC-00094-1)	1:200	RP	nucl	pos
EWS	Santa Cruz (clone G5)	1:200	MM	nucl > cyto	pos
	Bethyl Laboratories (IHC-00086)	1:200	RP	nucl > cyto	pos
hnRNP A1	Santa Cruz (clone 4B10)	1:500	MM	nucl	neg
hnRNP A0	Abcam (ab66661)	1:100	RP	nucl	neg
hnRNP A2/B1	Sigma-Aldrich (clone DP3B3)	1:500	MM	nucl	neg
hnRNP M3/M4	Santa Cruz (clone 2A6)	1:250	MM	nucl	neg
hnRNP D	ProteinTech Group (12770-1-AP)	1:500	RP	nucl	neg
hnRNP H1	ProteinTech Group (14774-1-AP)	1:50	RP	nucl > cyto	neg
PQBP-1	ProteinTech Group (16264-1-AP)	1:250	RP	nucl	neg
SAM68	ProteinTech Group (10222-1-AP)	1:250	RP	nucl	neg
SLM-2	ProteinTech Group (13563-1-AP)	1:50	RP	nucl	neg
HEXIM1	ProteinTech Group (15676-1-AP)	1:50	RP	nucl	neg
RBM39	ProteinTech Group (21339-1-AP)	1:50	RP	nucl > cyto	neg
HuR	Santa Cruz (clone 3A2)	1:250	MM	nucl	neg
PABPN1	Abcam (EP3000Y)	1:1,000	RM	nucl	neg

Cyto cytoplasmatic, *MM* mouse monoclonal, *nucl* nuclear, *pos* positive, *RP* rabbit polyclonal, *RM* rabbit monoclonal, *neg* negative

immunoreactivity of nuclei and weak diffuse cytoplasmic immunoreactivity in neurons (Fig. 1a).

In all subtypes of FTLD-FUS, Trn1 IHC revealed strong labeling of neuronal and glial inclusions (Table 1; Fig. 1b–g) with the frequency and morphology of inclusions being comparable to those demonstrated with FUS and TAF15 IHC. Antibodies against EWS labeled fewer inclusions, particularly in aFTLD-U, as previously described [27]. Specifically, aFTLD-U cases showed strong Trn1 staining of neuronal cytoplasmic inclusions (NCI) and neuronal intranuclear inclusions (NII) in the hippocampal dentate fascia (Fig. 1b, c) and the frontotemporal cortex. The numerous NCI in cortical, subcortical, brainstem and spinal cord regions in NIFID (Fig. 1d, g) and BIBD (Fig. 1e) cases were also strongly immunoreactive for Trn1. In addition to NCI, FTLD-FUS cases showed variable numbers of Trn1-positive glial cytoplasmic inclusions (GCI; Fig. 1f). The variability of physiological Trn1 immunoreactivity among cases mainly influenced by the time of tissue fixation did not allow a detailed quantification, but in cases with robust staining, inclusion bearing cells sometimes showed a clear reduction in nuclear Trn1 staining compared to cells without inclusions (Supplementary Fig. 1).

To confirm co-accumulation of Trn1 in the characteristic inclusions in FTLD-FUS with all FET proteins, we performed double-label immunohistochemistry for Trn1 and FUS, TAF15 or EWS of selected cases. This demonstrated consistent co-labeling of all Trn1-positive NCI and NII in cortical and spinal cord sections in aFTLD-U, NIFID and BIBD for FUS (Fig. 2a–c), and TAF15 (Supplementary Fig. 2). EWS and Trn1 co-localized in all inclusions in BIBD and NIFID cases, while in aFTLD-U only a subset of Trn1-positive inclusions was EWS immunoreactive (Supplementary Fig. 3).

Absence of Trn1 in inclusions in ALS with *FUS* mutations

Trn1 staining was investigated in six ALS-*FUS* cases with four different *FUS* mutations. All had previously been shown to have robust FUS-positive (but TAF15- and EWS-negative) pathology, particularly in the spinal cord and motor cortex, that included NCI and variable numbers of GCI [23]. In striking contrast to FTLD-FUS, no Trn1 immunoreactive neuronal or glial inclusions were detectable in cortical, subcortical, or spinal cord regions in any of the ALS-*FUS* cases, while the physiological nuclear staining pattern for Trn1 was retained (Fig. 1h). The absence of Trn1 accumulation in FUS-positive NCI and GCI in ALS-*FUS* was further confirmed by double-label IF (Fig. 3a–c).

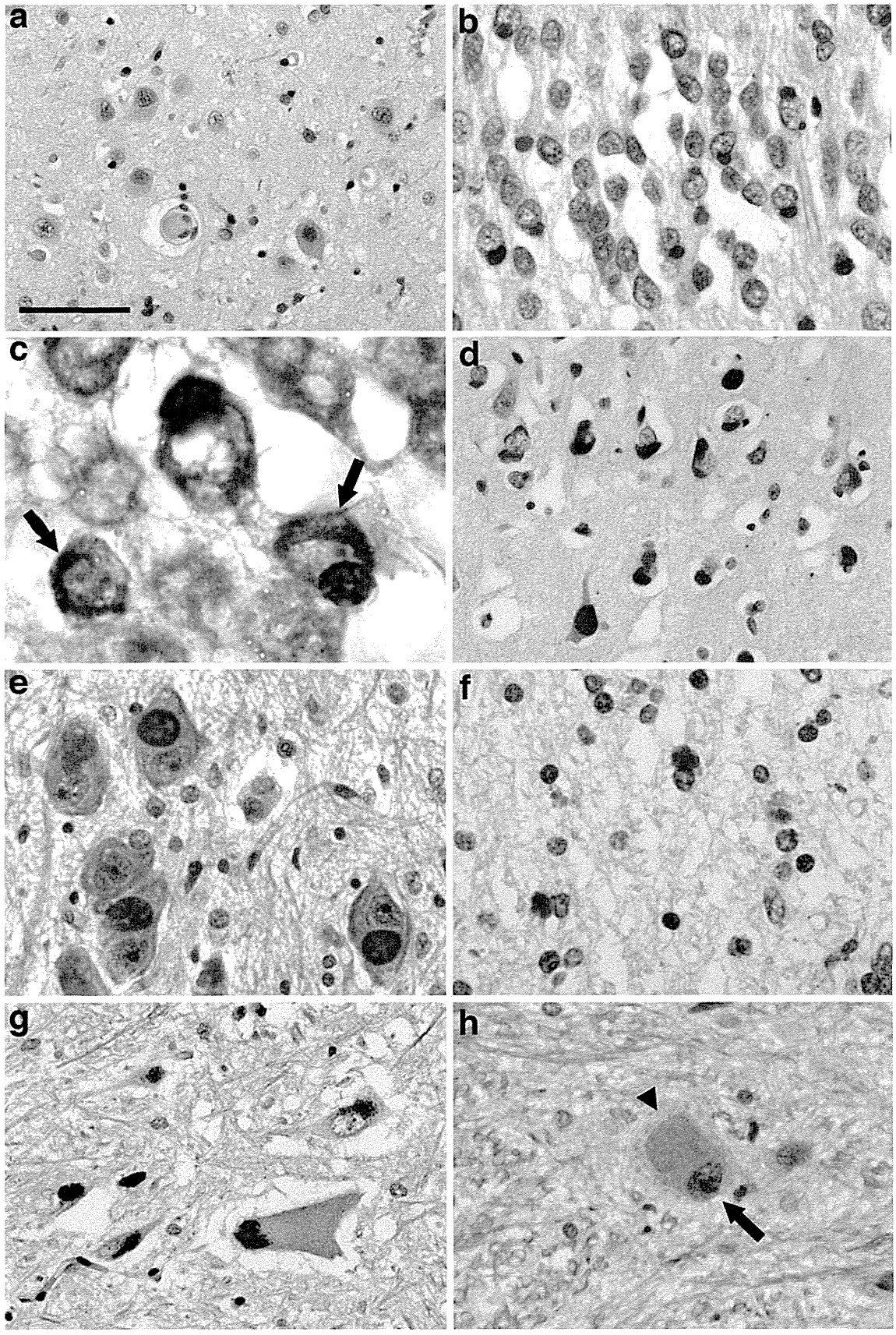
a
b
c
d
e
f
g
h

◀**Fig. 1** Trn1 immunohistochemistry in controls, FTLD-FUS and ALS-FUS. The physiological staining pattern of Trn1 consists of moderate to strong immunoreactivity of neuronal nuclei and weak diffuse cytoplasmic staining as shown in control cortex (**a**). Abundant Trn1-positive pathology is present in all affected brain regions in FTLD-FUS cases (**b–g**), including neuronal cytoplasmic inclusions (NCI) in the hippocampus in aFTLD-U (**b**, **c**), the neocortex (**d**) and spinal cord (**g**) in NIFID and the pons in BIBD (**e**). In addition to NCI, round and vermiform neuronal intranuclear inclusions (NII) were labeled in cases of aFTLD-U and NIFID (*arrows* in **c**) and glial cytoplasmic inclusions were present in the cerebral white matter (**f**). In striking contrast to FTLD-FUS, no Trn1 positive pathology was seen in ALS-*FUS* cases as shown for the spinal cord of the p.[R514S/;E516V] mutation (**h**); note the absence of Trn1 immunoreactivity of the basophilic inclusion (*arrowhead* in **h**) while nuclear staining is retained (*arrow* in **h**). *Scale bar* 125 μm (**a**), 63 μm (**b**, **e**, **h**), 20 μm (**c**), 90 μm (**d**, **g**), 45 μm (**f**)

Trn1 staining in neurological controls

The normal and neurological control cases did not reveal Trn1 immunoreactive pathology with one exception (Table 2). Specifically, there was no labeling of the characteristic inclusions in AD, FTLD-tau, FTLD-TDP, ALS-TDP, ALS-*SOD1,* and MSA. The exception was weak labeling of a subset of classical Lewy bodies in the substantia nigra in 7 of 8 PD cases with a frequency ranging from 2 to 14 %. Notably, NII in SCA, HD and NIIBD, which have previously been shown to be consistently FUS positive and more variably EWS positive [6, 27, 38], were negative for Trn1; a finding which further underlines the specificity of FET and Trn1 immunoreactive inclusions in FTLD-FUS.

Biochemical analysis of Trn1 in FTLD-FUS

To investigate potential biochemical alterations of Trn1 which might explain its co-accumulation in FTLD-FUS, proteins were sequentially extracted from frozen brain tissue from FTLD-FUS, as well as normal and neurological controls, using the same extraction protocol previously used to demonstrate changes in the solubility of FET protein as consistent biochemical alteration in FTLD-FUS [25, 27, 28].

Trn1 could be detected as major band at the expected molecular mass of ~97 kDa, in the HS, Triton-X, RIPA and SDS fractions in FTLD-FUS, as well as controls but not in the formic acid fraction enriched for highly insoluble

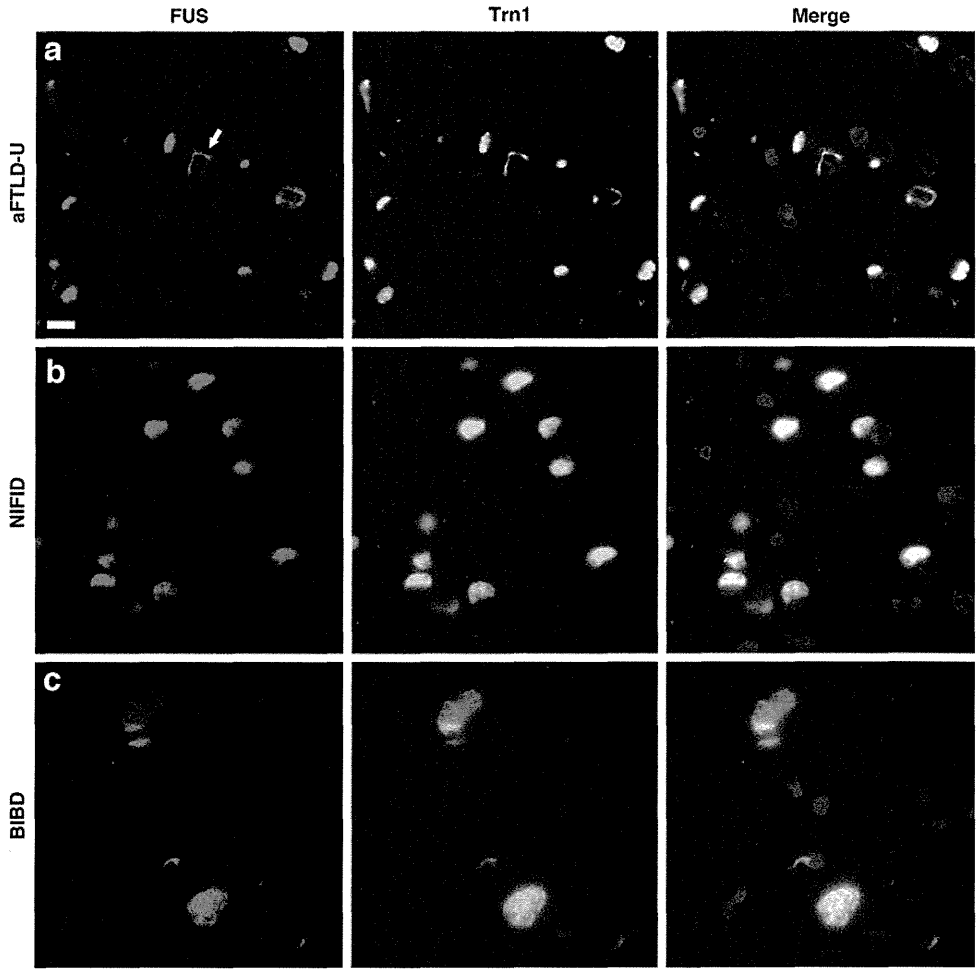

Fig. 2 Co-localization of Trn1 and FUS in all FTLD-FUS subtypes. Double-label immunofluorescence for FUS (*red*) and Trn1 (*green*), with DAPI staining of nuclei in the merged images. FUS-positive inclusions in all FTLD-FUS subtypes consistently showed co-localization of FUS and Trn1, as shown for neuronal cytoplasmic inclusions (NCI) and neuronal intranuclear inclusions (NII, *arrow* in **a**) in the dentate granule cells in aFTLD-U (**a**), NCI in the temporal cortex of NIFID (**b**) and NCI and glial cytoplasmic inclusions in the spinal cord of BIBD (**c**). *Scale bar* 10 μm

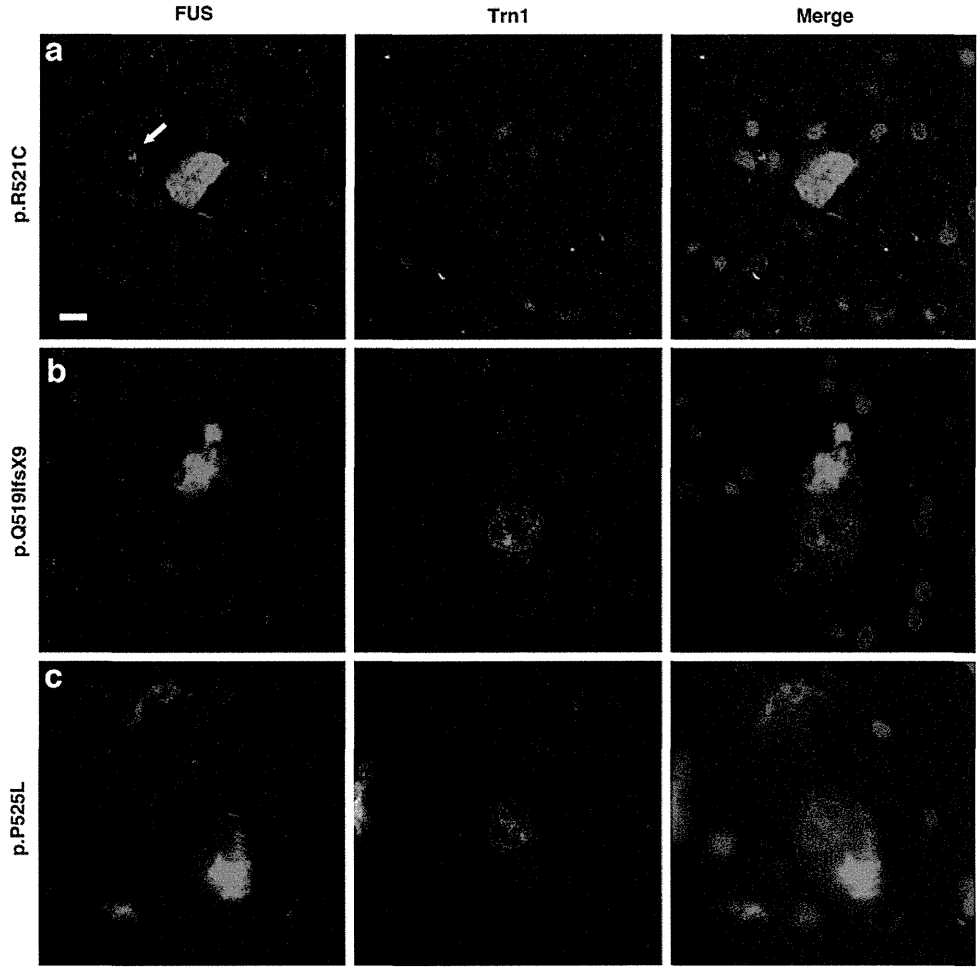

Fig. 3 Absence of Trn1 pathology in ALS-*FUS*. Double-label immunofluorescence for FUS (*red*) and Trn1 (*green*), with DAPI staining of nuclei in the merged images. FUS-positive inclusions in ALS-*FUS* were not labeled for Trn1 as shown for neuronal cytoplasmic inclusions in the spinal cord for three different *FUS* mutations (**a**–**c**). Note the physiological nuclear staining for Trn1 in inclusion bearing cells. FUS-positive glial cytoplasmic inclusions present in a subset of ALS-*FUS* cases also showed no co-labeling for Trn1 (*arrow* in **a**). *Scale bar* 10 μm

proteins (Fig. 4). There was some variability in the signal intensities between the different fractions among the various cases and controls; however, no consistent changes such as a shift in Trn1 solubility or additional Trn1 isoforms were observed in FTLD-FUS compared to controls. As positive control and validation of the extraction protocol, the same protein fractions were analyzed by immunoblot for FUS (Fig. 4), demonstrating a clear shift of FUS from the soluble HS fraction towards the insoluble SDS fraction in all FTLD-FUS cases compared to control cases, in accordance with previous reports.

Absence of other PY-NLS proteins in inclusions in FTLD-FUS

The co-accumulation of all FET proteins together with Trn1 in FTLD-FUS suggests a complex impairment of Trn1-mediated nuclear import in FTLD-FUS pathogenesis, raising the possibility that besides FET proteins other Trn1 cargo proteins might also be affected in FTLD-FUS. In order to test this hypothesis, we performed an immunohistochemical analysis of FTLD-FUS cases for 13 additional PY-NLS proteins (Table 3) described as validated cargo proteins of Trn1 [8, 18, 33]. IHC for all showed a predominantly nuclear staining pattern that was robust in neurons and weaker in glial cells in controls as well as FTLD-FUS cases. However, none of the antibodies against the additional PY-NLS proteins labeled inclusions in FTLD-FUS and no change in their normal physiological nuclear staining was observed in inclusion bearing cells. The absence of labeling of inclusions was confirmed by double-label immunofluorescence as illustrated for hnRNP A1, the best-characterized substrate of Trn1 (Fig. 5a), SAM68 (Fig. 5b), and PABPN1 (Fig. 5c).

Discussion

FUS accumulation characterizes all cases of ALS with *FUS* mutations and a variety of FTLD subtypes, collectively referred to as FTLD-FUS [15, 19, 24–26, 37]; however, the mechanisms of neurodegeneration in FUS-opathies are only poorly understood.

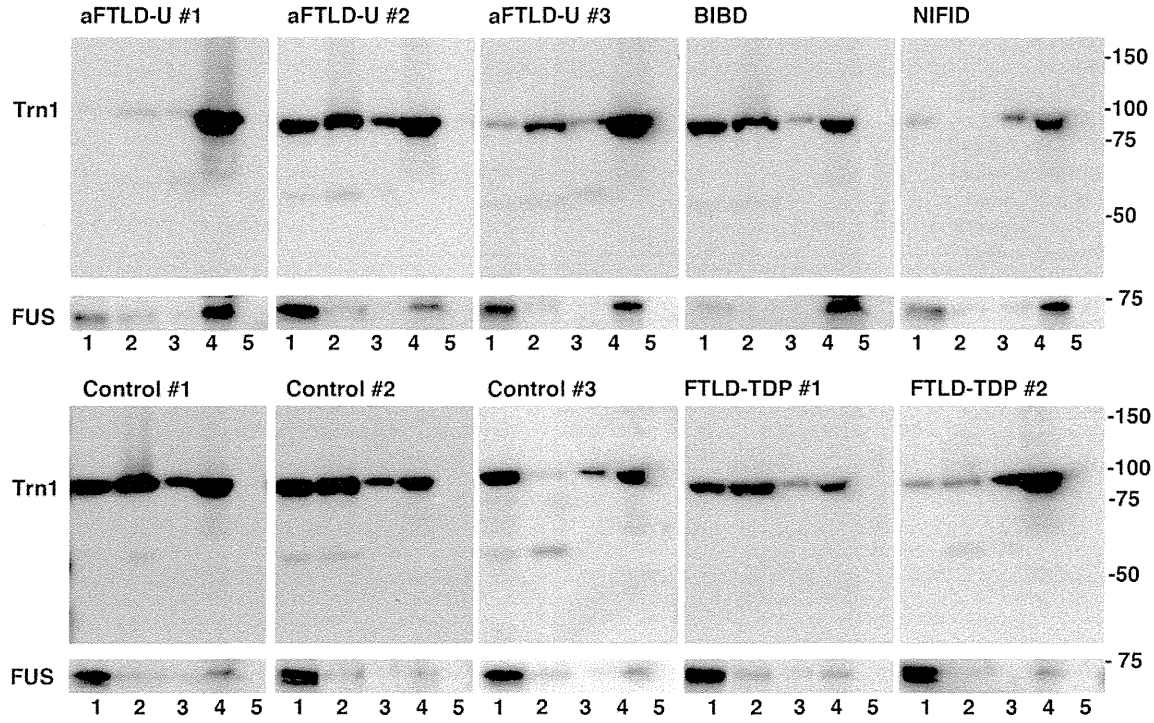

Fig. 4 Biochemical analysis of Trn1 and FUS in FTLD-FUS. Proteins were sequentially extracted from frontal cortex of aFTLD-U, NIFID, BIBD, controls without neurodegenerative disease as well as FTLD-TDP as neurological controls. High-salt (fraction 1), Triton-X-100 (fraction 2), RIPA (fraction 3), 2 % SDS (fraction 4) and formic acid (fraction 5) protein fractions were separated by SDS-PAGE and immunoblotted. Trn1 was present as one major band at the expected molecular size for the full-length protein (~97 kDa) in fractions 1–4 in FTLD-FUS and controls and was absent in fraction 5 enriched for highly insoluble proteins. While there was some variability among signal intensities in the different fractions among cases, no clear correlation of a distinct pattern was detectable in FTLD-FUS compared to controls. For validation of protein extractions, samples were analyzed by anti-FUS immunoblot, demonstrating full-length FUS at a molecular size of ~73 kDa with the amount of FUS present in the SDS fraction (fraction 4) being much higher in FTLD-FUS cases compared to controls, in accordance with previous reports

Based on our recent findings on differences in the protein composition of inclusions between ALS-*FUS* and FTLD-FUS with respect to the co-accumulation of the FUS homologues EWS and TAF15 [27], the hypothesis has emerged that these conditions might have different underlying pathomechanisms. The abnormality in ALS-*FUS* is restricted to alterations and dysfunction of FUS that result from *FUS* mutations that disrupt its PY-NLS and thereby interfere with proper binding to its nuclear transport receptor Trn1 and consecutive cytoplasmic accumulation of FUS, but not TAF15 and EWS [7, 27]. In contrast, FTLD-FUS is associated with accumulation of all FET proteins, thereby suggesting a broader defect of nuclear import pathways [5, 27], although the mechanism(s) of FET accumulation in the absence of mutations in their PY-NLS remain unclear.

Data presented in this study provide further strong evidence for different underlying mechanisms of inclusion body formation in ALS-*FUS* and FTLD-FUS by expanding the differences in the protein composition of inclusions between ALS-FUS and FTLD-FUS to Trn1.

None of the six ALS-*FUS* cases investigated (including three different FUS missense and one truncation mutations) showed alterations in the physiological staining pattern of Trn1 or evidence for co-accumulation of Trn1 in the FUS-positive neuronal and glial inclusions. Thus, the impaired binding capability of FUS with a mutated PY-NLS to Trn1 [7] is not associated with detectable changes in the subcellular distribution of Trn1 by IHC, which is also reflected by the unaffected nuclear import of other Trn1 cargo proteins such as TAF15 and EWS in ALS-*FUS* [27]. Thus, the absence of Trn1 pathology in ALS-*FUS* is consistent with the hypothesis that the pathological processes underlying ALS-*FUS* are restricted to dysfunctions of FUS.

In striking contrast to ALS-*FUS*, we demonstrate robust and consistent co-accumulation of Trn1 with all FET proteins in the various types of inclusions (NCI, GCI and NII) in our large collection of FTLD-FUS cases, including 17 aFTLD-U, 8 BIBD and 4 NIFID cases, in accordance with previous reports in smaller series of FTLD-FUS [4, 5]. Accumulation of Trn1 into cytoplasmic inclusions was

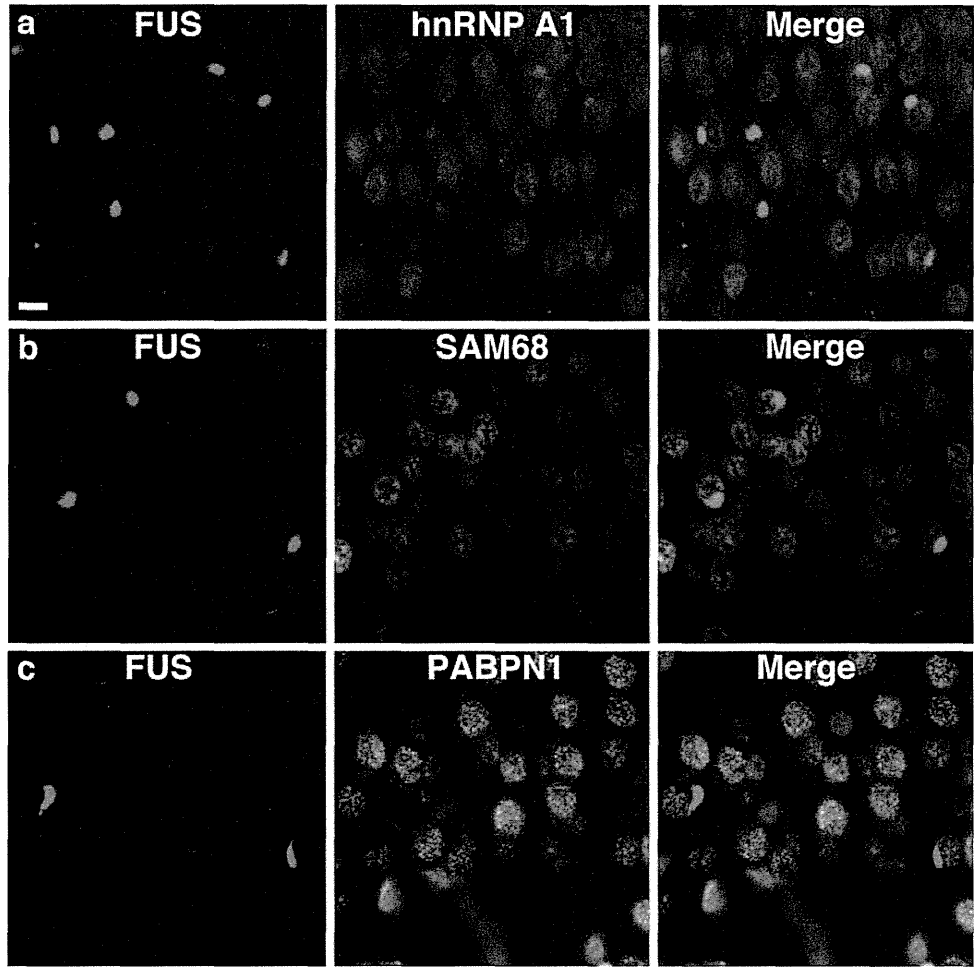

Fig. 5 Absence of selected other Trn1 cargos (hnRNP A1, SAM68 and PABPN1) in FTLD-FUS. Double-label immunofluorescence for FUS (*red*) and other Trn1 cargos with PY-NLS (hnRNP A1, SAM68 and PABPN1, respectively, *green*) with DAPI staining of nuclei in the merged images in FTLD-FUS. FUS-positive inclusions in FTLD-FUS as shown here in the dentate gyrus of aFTLD-U were not labeled for hnRNP A1 (**a**), SAM68 (**b**) and PABPN1 (**c**). *Scale bar* 10 μm

often associated with a reduction in the physiological nuclear staining of Trn1 in FTLD-FUS. Notably, the co-labeling of inclusions for Trn1 and all FET proteins was found to be a highly specific and unique feature of all subtypes of FTLD-FUS that was not present in any of our neurological controls, including those (HD, SCA, NIIBD) characterized by FUS and variable EWS immunoreactive NII [6, 27, 38]. These findings support the concept that aFTLD-U, NIFID and BIBD are closely related disease entities sharing the same pathomechanism [21]. Interestingly, a small subset of LBs in the midbrain of PD cases was found to be weakly positive for Trn1; however, the significance of this finding needs further investigation.

The dramatic changes in the subcellular distribution of Trn1 together with the accumulation of all FET proteins in FTLD-FUS support the idea of a complex dysregulation of Trn1-associated nuclear import in FTLD-FUS. This could result from a primary defect of Trn1 itself, either by posttranslational modifications, genetic variations or altered expression levels. In this scenario, one might expect to see changes of other Trn1 substrates and/or biochemical alterations Trn1 itself.

However, our immunohistochemical analysis of a large series of additional Trn1 cargo proteins failed to demonstrate any abnormal accumulation or alterations in their subcellular distribution. The Trn1 cargo proteins with PY-NLS motifs similar to FET proteins included in this study have all been validated in vitro as Trn1 binding proteins and included hnRNP A1, the best studied Trn1 cargo [8, 18, 33]. While we cannot exclude that some other PY-NLS proteins, in addition to FET proteins, might be affected in FTLD-FUS, our data strongly argue against a general dysfunction of Trn1 as a primary event in FTLD-FUS inclusion body formation. In line with that, we did not detect any specific biochemical alterations of Trn1 such as solubility changes or presence of abnormal Trn1 species in FTLD-FUS using a well-established sequential protein extraction protocol, able to reveal clear solubility changes for FUS, TAF15 and EWS in FTLD-FUS (this study, [25, 27]). However, our biochemical data are in disagreement with a previous publication describing a shift towards insolubility for Trn1 in aFTLD-U and NIFID [4]. This discrepancy might be due to different extraction protocols used, an issue which needs to be further addressed in future studies.

Based on our data we hypothesize an alternate scenario in which some abnormal posttranslational modification(s) that specifically affect FET proteins interferes with their normal Trn1 binding and dissociation and subsequently the proper nucleocytoplasmic transport of these shuttling proteins and their subcompartmental distribution in FTLD-FUS. Described posttranslational modifications of FET proteins include phosphorylation and arginine methylation and these have been shown to affect the cellular distribution, RNA/DNA-binding ability, protein–protein interaction, and protein stability of FET proteins in vitro [1, 2, 12, 30, 34, 35]. Beside changes in solubility of FET proteins [25, 27, 28], no disease-associated posttranslational changes have yet been reported in FTLD-FUS; however, this requires more detailed characterization. Notably, arginine methylation of FUS has been recently reported to weaken its interaction with Trn1 [8]. Together with the findings of co-accumulation of Trn1 in inclusions in FTLD-FUS, it is tempting to speculate that a reduced methylation status of FET proteins might be present in FTLD-FUS which would lead to a very tight binding to Trn1, thus hampering the normal dissociation of the transport complex resulting in co-accumulation of Trn1 and FET proteins in cytoplasmic and nuclear inclusions.

In summary, we have demonstrated striking differences in the accumulation of Trn1 in the spectrum of FUS-opathies with consistent Trn1 accumulation in FTLD-FUS but not in ALS-*FUS*, thereby providing further strong evidence for different mechanisms underlying inclusion body formation in FTLD-FUS and ALS-*FUS*. Notably, despite the dramatic changes in the subcellular distribution of Trn1 in FTLD-FUS, alterations of its cargo proteins were found to be restricted to FET proteins in FTLD-FUS, implying a specific dysfunction in the interaction between Trn1 and all FET proteins, most likely by posttranslational modifications of FET proteins, in the pathogenesis of FTLD-FUS.

Acknowledgments We thank Margaret Luk and Jay Tracy for their excellent technical assistance. This work was supported by grants from the Swiss National Science Foundation (31003A-132864, MN); the Synapsis Foundation (MN); the Canadian Institutes of Health Research (74580 and 179009, IM), the Pacific Alzheimer's Research Foundation (C06-01, IM); and the NIHR Oxford Biomedical Research Centre (OA).

References

1. Belyanskaya LL, Gehrig PM, Gehring H (2001) Exposure on cell surface and extensive arginine methylation of Ewing sarcoma (EWS) protein. J Biol Chem 276:18681–18687
2. Belyanskaya LL, Delattre O, Gehring H (2003) Expression and subcellular localization of Ewing sarcoma (EWS) protein is affected by the methylation process. Exp Cell Res 288:374–381
3. Blair IP, Williams KL, Warraich ST et al (2010) FUS mutations in amyotrophic lateral sclerosis: clinical, pathological, neurophysiological and genetic analysis. J Neurol Neurosurg Psychiatry 81:639–645
4. Brelstaff J, Lashley T, Holton JL et al (2011) Transportin1: a marker of FTLD-FUS. Acta Neuropathol 122:591–600
5. Davidson YS, Robinson AC, Hu Q et al (2012) Nuclear carrier and RNA binding proteins in frontotemporal lobar degeneration associated with fused in sarcoma (FUS) pathological changes. Neuropathol Appl Neurobiol. doi:10.1111/j.1365-2990.2012.01274.x
6. Doi H, Koyano S, Suzuki Y, Nukina N, Kuroiwa Y (2010) The RNA-binding protein FUS/TLS is a common aggregate-interacting protein in polyglutamine diseases. Neurosci Res 66:131–133
7. Dormann D, Rodde R, Edbauer D et al (2010) ALS-associated fused in sarcoma (FUS) mutations disrupt Transportin-mediated nuclear import. EMBO J 29:2841–2857
8. Fronz K, Guttinger S, Burkert K et al (2011) Arginine methylation of the nuclear poly(a) binding protein weakens the interaction with its nuclear import receptor, transportin. J Biol Chem 286:32986–32994
9. Groen EJ, van Es MA, van Vught PW et al (2010) FUS mutations in familial amyotrophic lateral sclerosis in the Netherlands. Arch Neurol 67:224–230
10. Hewitt C, Kirby J, Highley JR et al (2010) Novel FUS/TLS mutations and pathology in familial and sporadic amyotrophic lateral sclerosis. Arch Neurol 67:455–461
11. Ito D, Seki M, Tsunoda Y, Uchiyama H, Suzuki N (2010) Nuclear transport impairment of amyotrophic lateral sclerosis-linked mutations in FUS/TLS. Ann Neurol 69(1):152–162
12. Jobert L, Argentini M, Tora L (2009) PRMT1 mediated methylation of TAF15 is required for its positive gene regulatory function. Exp Cell Res 315:1273–1286
13. Kino Y, Washizu C, Aquilanti E et al (2011) Intracellular localization and splicing regulation of FUS/TLS are variably affected by amyotrophic lateral sclerosis-linked mutations. Nucleic Acids Res 39:2781–2798
14. Kovar H (2011) Dr. Jekyll and Mr. Hyde: the two faces of the FUS/EWS/TAF15 Protein Family. Sarcoma 837474. doi:10.1155/2011/837474
15. Kwiatkowski TJ Jr, Bosco DA, Leclerc AL et al (2009) Mutations in the FUS/TLS gene on chromosome 16 cause familial amyotrophic lateral sclerosis. Science 323:1205–1208
16. Lashley T, Rohrer JD, Bandopadhyay R et al (2011) A comparative clinical, pathological, biochemical and genetic study of fused in sarcoma proteinopathies. Brain 134:2548–2564
17. Law WJ, Cann KL, Hicks GG (2006) TLS, EWS and TAF15: a model for transcriptional integration of gene expression. Brief Funct Genomic Proteomic 5:8–14
18. Lee BJ, Cansizoglu AE, Suel KE et al (2006) Rules for nuclear localization sequence recognition by karyopherin beta 2. Cell 126:543–558
19. Mackenzie IR, Neumann M, Bigio EH et al (2010) Nomenclature and nosology for neuropathologic subtypes of frontotemporal lobar degeneration: an update. Acta Neuropathol 119:1–4
20. Mackenzie IR, Rademakers R, Neumann M (2010) TDP-43 and FUS in amyotrophic lateral sclerosis and frontotemporal dementia. Lancet Neurol 9:995–1007
21. Mackenzie IR, Munoz DG, Kusaka H et al (2011) Distinct pathological subtypes of FTLD-FUS. Acta Neuropathol 121:207–218
22. Mackenzie IR, Neumann M, Baborie A et al (2011) A harmonized classification system for FTLD-TDP pathology. Acta Neuropathol 122:111–113

23. Mackenzie IRA, Ansorge O, Strong M et al (2011) Pathological heterogeneity in amyotrophic lateral sclerosis with FUS mutations: two distinct patterns correlating with disease severity and mutation. Acta Neuropathol 122:87–98
24. Munoz DG, Neumann M, Kusaka H et al (2009) FUS pathology in basophilic inclusion body disease. Acta Neuropathol 118:617–627
25. Neumann M, Rademakers R, Roeber S et al (2009) A new subtype of frontotemporal lobar degeneration with FUS pathology. Brain 132:2922–2931
26. Neumann M, Roeber S, Kretzschmar HA et al (2009) Abundant FUS-immunoreactive pathology in neuronal intermediate filament inclusion disease. Acta Neuropathol 118:605–616
27. Neumann M, Bentmann E, Dormann D et al (2011) FET proteins TAF15 and EWS are selective markers that distinguish FTLD with FUS pathology from amyotrophic lateral sclerosis with FUS mutations. Brain 134:2595–2609
28. Page T, Gitcho MA, Mosaheb S et al (2011) FUS immunogold labeling TEM analysis of the neuronal cytoplasmic inclusions of neuronal intermediate filament inclusion disease: a frontotemporal lobar degeneration with FUS proteinopathy. J Mol Neurosci 45:409–421
29. Rademakers R, Stewart H, DeJesus-Hernandez M et al (2010) FUS gene mutations in familial and sporadic amyotrophic lateral sclerosis. Muscle Nerve 42:170–176
30. Rappsilber J, Friesen WJ, Paushkin S, Dreyfuss G, Mann M (2003) Detection of arginine dimethylated peptides by parallel precursor ion scanning mass spectrometry in positive ion mode. Anal Chem 75:3107–3114
31. Rohrer JD, Lashley T, Holton J et al (2011) The clinical and neuroanatomical phenotype of FUS associated frontotemporal lobar degeneration. J Neurol Neurosurg Psychiatry 82:1405–1407
32. Snowden JS, Hu Q, Rollinson S et al (2011) The most common type of FTLD-FUS (aFTLD-U) is associated with a distinct clinical form of frontotemporal dementia but is not related to mutations in the FUS gene. Acta Neuropathol 122:99–110
33. Suel KE, Gu H, Chook YM (2008) Modular organization and combinatorial energetics of proline-tyrosine nuclear localization signals. PLoS Biol 6:e137
34. Tan AY, Manley JL (2009) The TET family of proteins: functions and roles in disease. J Mol Cell Biol 1:82–92
35. Tradewell ML, Yu Z, Tibshirani M et al (2012) Arginine methylation by PRMT1 regulates nuclear-cytoplasmic localization and toxicity of FUS/TLS harbouring ALS-linked mutations. Hum Mol Genet 21:136–149
36. Urwin H, Josephs KA, Rohrer JD et al (2010) FUS pathology defines the majority of tau- and TDP-43-negative frontotemporal lobar degeneration. Acta Neuropathol 120:33–41
37. Vance C, Rogelj B, Hortobagyi T et al (2009) Mutations in FUS, an RNA processing protein, cause familial amyotrophic lateral sclerosis type 6. Science 323:1208–1211
38. Woulfe J, Gray DA, Mackenzie IR (2010) FUS-immunoreactive intranuclear inclusions in neurodegenerative disease. Brain Pathol 20:589–597
39. Zakaryan RP, Gehring H (2006) Identification and characterization of the nuclear localization/retention signal in the EWS proto-oncoprotein. J Mol Biol 363:27–38
40. Zinszner H, Sok J, Immanuel D, Yin Y, Ron D (1997) TLS (FUS) binds RNA in vivo and engages in nucleo-cytoplasmic shuttling. J Cell Sci 110:1741–1750

Med Mol Morphol (2012) 45:86–90
DOI 10.1007/s00795-011-0542-7

ORIGINAL PAPER

Seika Nakamura · Satoshi Nakano · Makoto Nishii
Satoshi Kaneko · Hirofumi Kusaka

Localization of *O*-GlcNAc-modified proteins in neuromuscular diseases

Received: December 20, 2010 / Accepted: February 18, 2011

Abstract O-linked *N*-acetylglucosamine (*O*-GlcNAc) is a ubiquitous post-translational modification of nucleocytoplasmic proteins that induces the attachment of *N*-acetylglucosamine to serine or threonine residues of a protein. In contrast to other protein glycosylations, this modification is highly reversible and, similar to phosphorylation, it plays important roles in various cell signals. Here, we immunolocalized *O*-GlcNAc-modified proteins in muscle biopsy specimens from 40 patients with neuromuscular diseases and controls. In normal muscle fibers, *O*-GlcNAc was found along plasma membranes and in nuclei. Diffuse and increased cytoplasmic staining of *O*-GlcNAc was detected in (1) regenerating muscle fibers in muscular dystrophy, myositis, and rhabdomyolysis; (2) a proportion of atrophic fibers in myositis, such as those found in perifascicular regions in dermatomyositis; and (3) vacuolated fibers in sporadic inclusion body myositis (s-IBM) and distal myopathy with rimmed vacuoles (DMRV). Target formations in neurogenic muscular atrophy were *O*-GlcNAc positive. Increase of *O*-GlcNAc glycosylation could be associated with the stress response, as these lesions have been shown to be positive for several stress markers. Vacuolar rims in s-IBM and DMRV were sometimes sharply lined by *O*-GlcNAc-positive deposits, which reflects myonuclear breakdown occurring from the disease.

Key words O-linked *N*-acetylglucosamine (*O*-GlcNAc) · Skeletal muscle · Neuromuscular diseases · Myositis · Rimmed vacuoles · Glycosylation

S. Nakamura · S. Nakano · M. Nishii · S. Kaneko · H. Kusaka
Department of Neurology and Brain Medical Research Center, Kansai Medical University, Osaka, Japan

S. Nakano (✉)
Department of Neurology, Osaka City General Hospital, 2-13-22 Miyakojima Hondori, Miyakojima-ku, Osaka 534-0021, Japan
Tel. +81-6-6929-1221; Fax +81-6-6929-1091
e-mail: s-nakano@hospital.city.osaka.jp; nakanos@takii.kmu.ac.jp

A part of this study has been presented at the 50th Annual Meeting of the Japanese Society of Neurology (Sendai, May 2009).

Introduction

O-linked *N*-acetylglucosamine, termed *O*-GlcNAc, is a key post-translational modification that occurs in nuclear and cytoplasmic proteins, consisting of the addition of a unique monosaccharide, *N*-acetylglucosamine, to a serine/threonine hydroxyl group of a protein. *O*-GlcNAc has been implicated in the regulation of more than 500 intracellular proteins, including chaperones, cytoskeletal components, kinases and metabolic enzymes, hormone receptors, nuclear pore proteins, and transcription factors.[1] Many studies indicate that *O*-GlcNAc acts as a modulator of protein function, in a manner more analogous to protein phosphorylation than to classical glycosylation. Moreover, there is an extremely complex crosstalk between *O*-GlcNAc modification and phosphorylation. The two posttranslational modifications often regulate in a reciprocal manner by competitive attachment to the same serine/threonine residue, but they sometimes function cooperatively by binding at different sites of the same molecule.[2] *O*-GlcNAc modification is a highly dynamic process and is involved in various cellular signalings, such as the cell cycle, development, nuclear transport, glucose metabolism, and cellular stress.

O-GlcNAc modification of nucleocytoplasmic protein swiftly increases in response to a wide variety of stress stimuli, such as heat shock, hypoxia, and oxidative stress. Blocking or reducing this modification renders cells more sensitive to stress and affects cell survival. Conversely, increasing *O*-GlcNAc levels protects cells. *O*-GlcNAc regulates both the rates and extent of the stress-induced induction of heat shock proteins.[3]

Immunohistochemical findings have shown the presence of a stress response evidenced by the detection of heat shock/chaperone proteins or markers of oxidative injuries in some muscle fibers in myositis and in other neuromuscular diseases.[4,5] Recent studies have shown *O*-GlcNAc modification in proteins in the skeletal muscle metabolism and contractile processes[6]; however, the localization of *O*-GlcNAc in skeletal muscle and the alteration of *O*-GlcNAc in muscle diseases have not been studied.

In the present study, we examined the localization of *O*-GlcNAc-modified proteins in human skeletal muscle and their changes in neuromuscular diseases.

Materials and methods

We used 40 diagnostic muscle biopsies from patients with polymyositis (n = 7), dermatomyositis (6), sporadic inclusion body myositis (s-IBM) (7), muscular dystrophies (8), neurogenic muscular atrophy (5), rhabdomyolysis (1), and distal myopathy with rimmed vacuoles (3). Specimens from 3 patients without pathological alterations served as non-pathological controls. The foregoing diagnoses were based on a clinical examination, family history, electromyography, and muscle biopsy studies. Polymyositis and dermatomyositis were diagnosed using conventional criteria: polymyositis samples contained some to many nonnecrotic fibers surrounded by mononuclear cells, and dermatomyositis samples showed perifascicular atrophy or perimysial infiltration of inflammatory cells.[7] Patients with s-IBM fulfilled the criteria proposed by Griggs et al.: the muscle sections displayed cell infiltration surrounding nonnecrotic fibers, congophilic inclusions, and rimmed vacuoles in each patient.[8] This study was performed with the compliance of the internal review board of our institution.

Serial 7-μm cryostat sections were prepared from muscle samples stored in −85°C, fixed with cold acetone, and treated with blocking solution containing 5% horse serum, and 2% bovine serum albumin in phosphate-buffered saline, pH 7.4. Incubation with primary antibodies was performed in the same solution. We used well-characterized anti-*O*-GlcNAc antibody[9] (mouse monoclonal, clone RL-2; Affinity BioReagents, Golden, CO, USA, at 1:100 dilution. Immunostaining was completed using a biotinylated anti-mouse IgG developed in horse (Vector Laboratories, Burlingame, CA, USA), and the avidin–biotin complex (ABC) immunoperoxidase method (Vector Laboratories), visualized with 3,3′-diaminobenzidine. Controls included incubation with nonimmune mouse IgG at the same concentration. Regenerating fibers and other pathological changes were identified on conventional criteria[10] by visualizing serial sections stained with hematoxylin and eosin (H&E) and other routine histochemical staining for muscle biopsy. In selected patients, we examined the localization of heat shock protein 70 (HSP70) in the serial sections of *O*-GlcNAc staining using anti-HSP70 antibody (K-20; Santa Cruz Biotechnology, Santa Cruz, CA, USA).

For dual-color immunofluorescence studies, the sections were incubated with anti-*O*-GlcNAc plus anti-emerin (FL-254, rabbit polyclonal; Santa Cruz Biotechnology) antibodies followed by incubation with secondary antibodies for multiple fluorescence study (Chemicon International, Temecula, CA, USA). The slides were mounted with Vectashield (Vector Laboratories) and examined with confocal imaging using the LSM510-META system (Carl Zeiss, Jena, Germany). To confirm the specificity of the secondary antibodies and filters, we performed a single-color fluorescence study using each antibody.

Table 1. Summary of the results in the O-linked *N*-acetylglucosamine (*O*-GlcNAc) immunohistochemical study

Fibers	Plasma membrane	Cytoplasm	Nucleus
Normal	+	+/–	+
Regenerating	+/–	++	++
Necrotic	+/–	+/– to +	+
Hypertrophic	+ to ++	+/– to +	+
Atrophic fibers:			
In dystrophy	0 to +/–	+/–	+ to ++
In myositis	0 to +/–	+/– to ++	+ to ++
Small angulated[a]	0 to +/–	+/–	+ to ++
Vacuolated[b]	0 to +/–	+ to ++[c]	++

0, immunoreactivity absent ; +/–, weak *O*-GlcNAc immunoreactivity; +, intermediate *O*-GlcNAc immunoreactivity; ++, strong *O*-GlcNAc immunoreactivity

[a] Small angulated fibers in neurogenic muscular atrophy

[b] Fibers with rimmed vacuoles in sporadic inclusion body myositis and distal myopathy with rimmed vacuoles

[c] Some of the rimmed vacuoles displayed strong *O*-GlcNAc-positive deposits along the rims of the vacuoles

Results

In control studies with normal animal IgG, no immunoreactivity was detected in muscle sections, such as within atrophic fibers in myositis. Table 1 shows the summary of the results in the *O*-GlcNAc immunohistochemical study. Normal muscle fibers showed intermediate levels of *O*-GlcNAc staining along plasma membranes as well as in nuclei and low levels of *O*-GlcNAc in the cytoplasm (Fig. 1A). Some of the atrophic fibers in dystrophy, myositis, or neurogenic muscular atrophy were negative or weak in the sarcolemmal *O*-GlcNAc. Muscle biopsies from dystrophy or rhabdomyolysis patients showed increased *O*-GlcNAc staining in regenerating muscle fibers (Fig. 1B). Regenerating fibers and some scattered atrophic fibers in each type of myositis, and perifascicular atrophic fibers in dermatomyositis, displayed high levels of *O*-GlcNAc (Fig. 1C). Inflammatory cells infiltrating in myositis were *O*-GlcNAc positive. Target formations in neurogenic muscular atrophy showed increased *O*-GlcNAc staining (Fig. 1D). Vacuolated fibers in s-IBM and DMRV expressed increased *O*-GlcNAc content. Some of the vacuolar rims were strongly and sharply positive for *O*-GlcNAc (Fig. 2). In s-IBM (Fig. 3) and DMRV (data not shown), the fluorescence study showed that these *O*-GlcNAc-positive lines in vacuolar rims were also positive for emerin, which is an inner nuclear membrane protein.

The HSP70 immunolocalization study showed increased levels of HSP70 in the cytoplasm of regenerating fibers, perifascicular atrophic fibers (Fig. 4A), target formations, and vacuolated fibers in s-IBM (Fig. 4B) and DMRV (data not shown).

Discussion

Recent biochemical studies showed several *O*-GlcNAc-modified proteins associated with muscle metabolism and

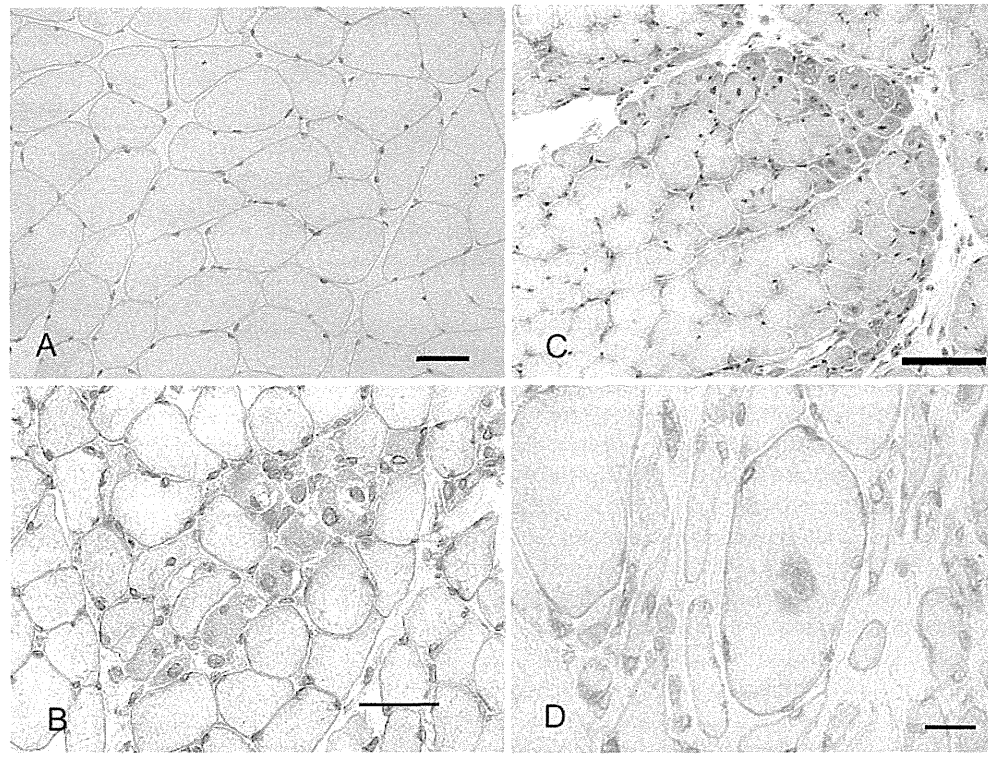

Fig. 1. Immunolocalization of O-linked *N*-acetylglucosamine (*O*-GlcNAc) in muscle biopsies. Peroxidase method. **A** Positive staining at plasma membranes and nuclei in normal muscle fibers. **B** Regenerating fibers, which represent small and round fibers with vesicular nuclei, are strongly positive in the cytoplasm (sample: rhabdomyolysis). **C** Perifascicular atrophic fibers in dermatomyositis showed increased cytoplasmic *O*-GlcNAc. All fibers in this image are atrophic, <60 μm in diameter, and negative for sarcolemmal *O*-GlcNAc. **D** Positive staining in target formations in neurogenic muscular atrophy. *Bars* **A** 50 μm; **B**, **C** 100 μm; **D** 20 μm

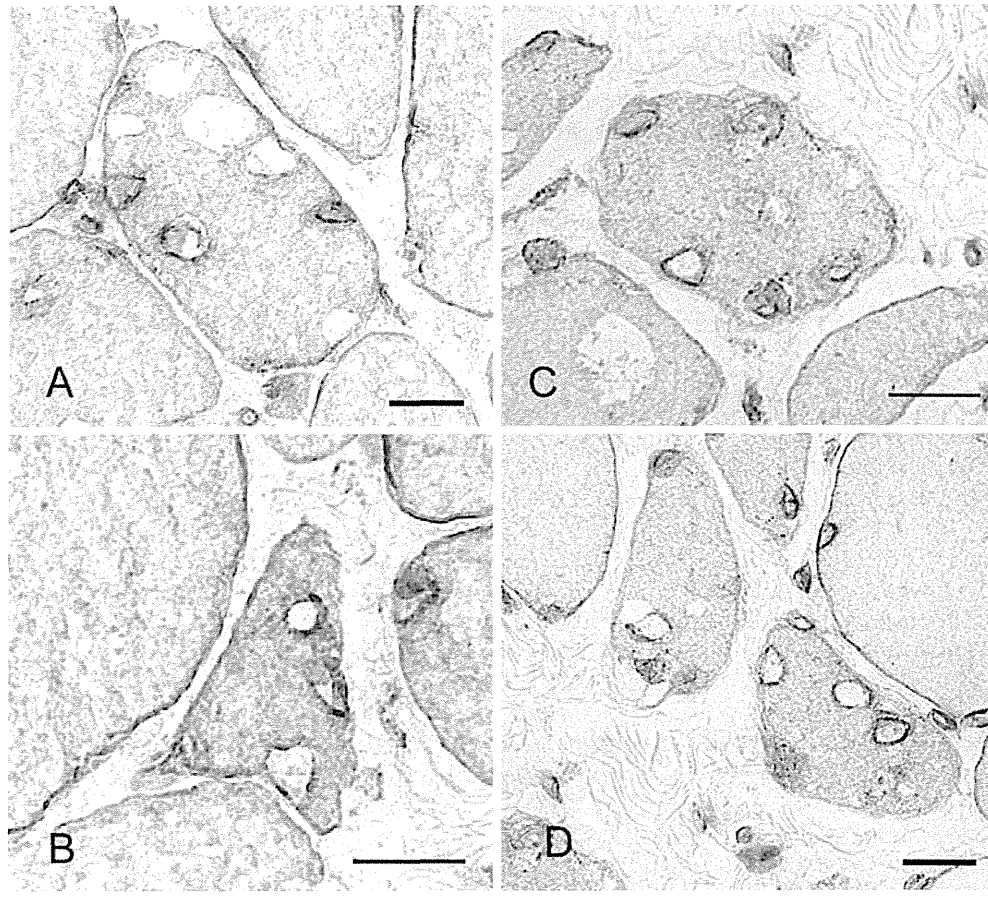

Fig. 2. Immunolocalization of *O*-GlcNAc in sporadic inclusion body myositis (s-IBM) (**A**, **B**) and distal myopathy with rimmed vacuoles (DMRV) (**C**, **D**). Vacuolated fibers display increased *O*-GlcNAc staining. Some of the vacuoles are encircled by *O*-GlcNAc-positive deposits. *Bars* 20 μm

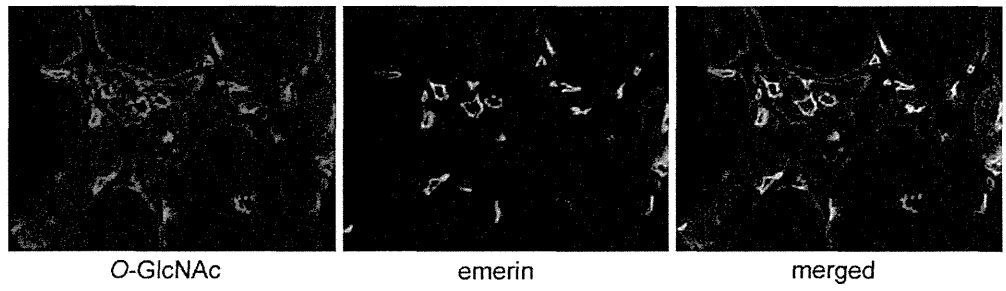

Fig. 3. Dual-color fluorescence study in vacuolated fibers observed in s-IBM. Along vacuolar rims, *O*-GlcNAc-positive lines or deposits (*red*) colocalize with emerin (*green*)

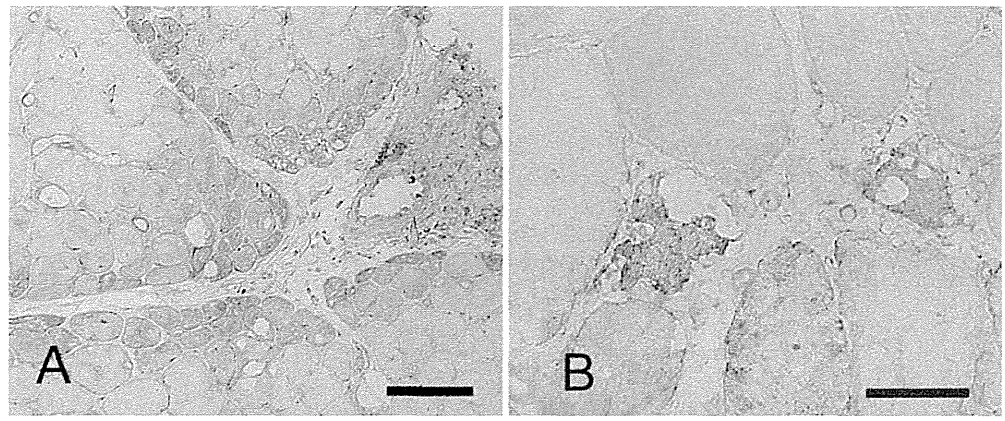

Fig. 4. Immunolocalization of heat shock protein (HSP)70 in dermatomyositis (**A**) and in s-IBM (**B**). **A** Perifascicular fibers show high levels of HSP70. **B** Vacuolated fibers display increased HSP70 signal. *Bars* **A** 100 μm; **B** 50 μm

contractile processes[6]; however, neither the localization of *O*-GlcNAc in skeletal muscle nor the alterations of *O*-GlcNAc in muscle diseases have been studied. In this article, we have shown that in skeletal muscle *O*-GlcNAc is concentrated on the plasma membrane and in the nucleus. *O*-GlcNAc on the plasma membrane may include proteins associated with the initiation of intracellular cell signaling cascades, such as those of insulin.[11] Many nuclear transcription factors and nuclear pore proteins are known to be *O*-GlcNAc modified, which may account for nuclear staining.[3]

In neuromuscular diseases, we observed high levels of cytoplasmic *O*-GlcNAc in regenerating fibers in various muscle diseases, and atrophic fibers in myositis as well as vacuolated fibers in s-IBM and DMRV. Target formations displayed increased *O*-GlcNAc staining. We also examined HSP70 in some serial sections of the *O*-GlcNAc-stained materials and found increased levels of cytoplasmic HSP70 in fibers with high cytoplasmic *O*-GlcNAc content. A study has examined HSP70 in myositis and, as our HSP70 study, found increases of HSP70 in the cytoplasm of regenerating fibers of myositis, atrophic perifascicular muscle fibers of dermatomyositis, and vacuolated fibers in s-IBM.[4] HSPs are stress proteins involved in protein metamorphosis and suppress the aggregation of misfolded proteins. Interestingly, HSP70 itself is an *O*-GlcNAc-modified protein and acts as lectin for *O*-GlcNAc upon stress.[12] In damaged fibers, *O*-GlcNAc protein modification could play a role in the stress response, together with HSP70.

The proposed mechanism of muscle fiber injury is T-cell-mediated muscle cell toxicity in polymyositis and s-IBM. Conversely, muscle fiber injury may be caused by complement-mediated endotheliopathy in dermatomyositis.[7] The endoplasmic reticulum (ER) stress response, induced by the overexpression of major histocompatibility complex (MHC)-I, may be evoked in myositis muscle fibers.[5] Vacuolated fibers in s-IBM and DMRV have been shown to be under nitric oxide-induced oxidative stress.[13,14] Target formations are a sign of reinnervation.[15] Such myocyte stresses could be involved in the induction of *O*-GlcNAc glycosylation.

Nuclear remnants have been detected in rimmed vacuoles in s-IBM and DMRV, indicating that nuclear breakdown results in vacuoles.[16] The nucleus-like contour, circular or comma-shaped *O*-GlcNAc staining co-localized with emerin, could be nuclear envelope proteins including nucleoporins that represent the protein family modified by *O*-GlcNAc.[17] A mutation of the UDP-*N*-acetylglucosamine 2-epimerase/*N*-acetylmannosamine kinase (GNE) gene causes DMRV.[18] The GNE protein is an enzyme involved in a glycosylation cascade and the substrate of GNE is UDP-*N*-acetylglucosamine. Interestingly, UDP-*N*-acetylglucosamine is also the substrate of O-linked *N*-actetylglucosamine transferases (OGT), which catalyze *O*-GlcNAc modification. In DMRV, abnormal GNE function could perturb the UDP-*N*-acetylglucosamine reservoir, thus affecting *O*-GlcNAc modifications of nuclear proteins. It would be necessary to study whether and how abnormal nuclear *O*-GlcNAc modifications can induce nuclear breakdown.

Conclusion

We immunolocalized *O*-GlcNAc-modified proteins in normal and affected muscles. The identification and analysis

of *O*-GlcNAc-modified proteins in neuromuscular diseases could provide new insight into the stress response in the course of muscle cell degeneration.

Acknowledgments This work was supported by Grant-in-Aids from the Japan Society for the Promotion of Science and from the Ministry of Health, Labour, and Welfare for Research on intractable diseases.

References

1. Zachara NE, Hart GW (2004) *O*-GlcNAc a sensor of cellular state: the role of nucleocytoplasmic glycosylation in modulating cellular function in response to nutrition and stress. Biochim Biophys Acta 1673:13–28
2. Zeidan Q, Hart GW (2010) The intersections between O-GlcNAcylation and phosphorylation: implications for multiple signaling pathways. J Cell Sci 123:13–22
3. Zachara NE, O'Donnell N, Cheung WD, Mercer JJ, Marth JD, Hart GW (2004) Dynamic O-GlcNAc modification of nucleocytoplasmic proteins in response to stress. A survival response of mammalian cells. J Biol Chem 279:30133–30142
4. De Paepe B, Creus KK, Martin JJ, Weis J, De Bleecker JL (2009) A dual role for HSP90 and HSP70 in the inflammatory myopathies: from muscle fiber protection to active invasion by macrophages. Ann N Y Acad Sci 1173:463–469
5. Vitadello M, Doria A, Tarricone E, Ghirardello A, Gorza L (2010) Myofiber stress-response in myositis: parallel investigations on patients and experimental animal models of muscle regeneration and systemic inflammation. Arthritis Res Ther 12:R52
6. Hedou J, Cieniewski-Bernard C, Leroy Y, Michalski JC, Mounier Y, Bastide B (2007) O-linked N-acetylglucosaminylation is involved in the Ca^{2+} activation properties of rat skeletal muscle. J Biol Chem 282:10360–10369
7. Dalakas MC, Hohlfeld R (2003) Polymyositis and dermatomyositis. Lancet 362:971–982
8. Griggs RC, Askanas V, DiMauro S, Engel A, Karpati G, Mendell JR, Rowland LP (1995) Inclusion body myositis and myopathies. Ann Neurol 38:705–713
9. Walgren JL, Vincent TS, Schey KL, Buse MG (2003) High glucose and insulin promote O-GlcNAc modification of proteins, including alpha-tubulin. Am J Physiol Endocrinol Metab 284:E424–E434
10. Banker BQ, Engel AG (2004) Basic reactions of muscle. In: Engel AG, Franzini-Armstrong C (eds) Myology. McGraw-Hill, New York, pp 691–747
11. Whelan SA, Lane MD, Hart GW (2008) Regulation of the O-linked beta-*N*-acetylglucosamine transferase by insulin signaling. J Biol Chem 283:21411–21417
12. Guinez C, Mir AM, Leroy Y, Cacan R, Michalski JC, Lefebvre T (2007) Hsp70-GlcNAc-binding activity is released by stress, proteasome inhibition, and protein misfolding. Biochem Biophys Res Commun 361:414–420
13. Tsuruta Y, Furuta A, Taniguchi N, Yamada T, Kira J, Iwaki T (2002) Increased expression of manganese superoxide dismutase is associated with that of nitrotyrosine in myopathies with rimmed vacuoles. Acta Neuropathol 103:59–65
14. Yang CC, Alvarez RB, Engel WK, Askanas V (1996) Increase of nitric oxide synthases and nitrotyrosine in inclusion-body myositis. Neuroreport 8:153–158
15. Dubowitz V (1967) Pathology of experimentally re-innervated skeletal muscle. J Neurol Neurosurg Psychiatry 30:99–110
16. Nakano S, Shinde A, Fujita K, Ito H, Kusaka H (2008) Histone H1 is released from myonuclei and present in rimmed vacuoles with DNA in inclusion body myositis. Neuromuscul Disord 18:27–33
17. Miller MW, Caracciolo MR, Berlin WK, Hanover JA (1999) Phosphorylation and glycosylation of nucleoporins. Arch Biochem Biophys 367:51–60
18. Nishino I, Noguchi S, Murayama K, Driss A, Sugie K, Oya Y, Nagata T, Chida K, Takahashi T, Takusa Y, Ohi T, Nishimiya J, Sunohara N, Ciafaloni E, Kawai M, Aoki M, Nonaka I (1999) Distal myopathy with rimmed vacuoles is allelic to hereditary inclusion body myopathy. Neurology 59:1689–1693

生体の科学　63(5)：534-535，2012

封入体筋炎における核遺残物を含んだ空胞

中野　智　日下博文

●封入体筋炎とは

封入体筋炎は多発筋炎，皮膚筋炎と同じく骨格筋の炎症性疾患に分類される[1]。50歳以降に発症し，緩徐進行性で，典型的な例では手指筋と大腿四頭筋の選択的かつ著明な萎縮を示す。その発症には自己免疫学的機序が推定されているが，副腎皮質ステロイドなどによる治療に対する反応性が低いことが知られている。確定診断は筋生検で行われ，組織では多発筋炎と同様，筋線維周囲に細胞傷害性T細胞を中心とした炎症細胞浸潤像が見られる。加えて，縁取り空胞と呼ばれるヘマトキシリン-エオジン染色で青色すなわち好塩基性の物質により縁取りされた空胞が筋細胞質に存在する。好塩基性物質は空胞内に顆粒状に認められることもある。電子顕微鏡ではしばしば細胞質，ときに核にフィラメント構造の封入体が見られ，このことにより封入体筋炎の名称が与えられている。しかし，組織学的にはむしろ縁取り空胞が目立つ。本疾患は欧米では有病率が高く，治療抵抗性であることと合わせ，病態解明から治療に至る道が模索されている。

●縁取り空胞の好塩基性物質の正体

本疾患における病態解明の糸口の一つは，縁取り空胞の形成機序を明らかにすることと思われる。縁取り空胞は核由来であることを示唆するデータは以前からあったが，好塩基性物質が核の成分であることを直接証明した研究はなかった。核には好塩基性蛋白が多く含まれる。そのうち特にヒストンは強い好塩基性を示す。ヒストンはクロマチンを構成する蛋白で，DNAという非常に長い分子を核内に収容する役割を持っている。ヒストンは大きく5種類(H1，H2A，H2B，H3，H4)に分類される。このうちH2A，H2B，H3，H4の4種はコアヒストンといわれ，それぞれ二分子が集まり球状のヒストン八量体(ヒストンオクタマー)を形成する。一つのヒストンオクタマーにDNAが巻き付いたものはヌクレオソームと呼ばれ，クロマチンの最小単位である。H1は別名がリンカーヒストンで，ヌクレオソーム間のDNA(リンカーDNA)に結合する。H1はクロマチンの高次構造維持・可塑性と関連し，その挙動は遺伝子発現と密接にかかわる。われわれはこれらのヒストンが好塩基性物質の本体である可能性を検証するため，5種のヒストンそれぞれに対する特異抗体を用いて免疫組織学的に検討した。その結果，5種のヒストンのうちH1が空胞壁に陽性であった(図)。しかもヘマトキシリン-エオジン染色と比較したところ，H1や核DNAマーカーの分布と空胞壁の縁のヘマトキシリン陽性反応の分布はよく一致した[2]。したがって，空胞壁の好塩基性物質はH1をはじめとする核由来物質であると考えられた。また，正常に見える核から放射状に細胞質へと分布するH1陽性反応が一部に見られ，封入体筋炎の筋細胞核では核変性の初期にH1の核からの遊離が起こっていると推定された。

●封入体筋炎筋細胞におけるDNA二本鎖切断修復異常

封入体筋炎筋組織で観察されたような核から細胞質へH1が遊離する現象は，DNA二本鎖切断に伴って起こるという培養細胞での研究結果[3]をヒントに，われわれはさらに免疫組織学的に二本鎖切断やその修復酵素について免疫組織化学的に検討した[4]。DNA二本鎖切断の指標として，Ser

Satoshi Nakano：大阪市立総合医療センター 神経内科
Hirohumi Kusaka：関西医科大学 神経内科

139残基がリン酸化されたヒストンH2AX(γ-H2AX)，およびDNA二本鎖切断修復酵素であるDNA-PK構成蛋白のDNA-PKcs，Ku70，Ku80に対する抗体を用いて免疫組織学的検討を行った。その結果，封入体筋炎の変性した筋線維の核といくつかの空胞壁にγ-H2AXとDNA-PKの三つの構成蛋白の強い陽性反応が認められた。さらに，Ku70は細胞質と核の周囲に凝集体がしばしば見られた。免疫電顕ではKu70陽性物質を含むvesicleが細胞質内の空胞内，変性した核と思われる構造物の周囲に観察された。光顕では，封入体筋炎の空胞化線維における核のγ-H2AX陽性率は，非空胞化線維や多発筋炎の筋線維核のγ-H2AX陽性率より統計学的に有意に高値であった。したがって，封入体筋炎における空胞変性筋線維ではDNA二本鎖切断反応が亢進していると推定された。この亢進の原因としては，Ku70の核内への輸送障害などが原因となり，DNA二本鎖切断の修復障害が生じている可能性がある。また，DNA二本鎖切断反応の亢進・核の崩壊の原因の可能性の一つとして，自己免疫・炎症反応による酸化的ストレス・加齢などによって引き起こされた核膜の脆弱性があるものと推定した。

●封入体筋炎組織における核輸送障害

封入体筋炎では，ある種のリン酸化蛋白が筋細胞質に沈着することが知られていた。そのことから，われわれは蛋白リン酸化酵素，すなわちプロテインキナーゼを免疫組織学的に検討した。沈着するリン酸化蛋白はプロリン向性キナーゼでリン酸化されるような配列を持っていたため，それらのキナーゼのうちの代表的なサイクリン依存性キナーゼ(CDK1，CDK2，CDK4，CDK5)とMAPキナーゼ(ERK1/2，p38，JNK)を検討したところ，これらのうちCDK5とERK1/2が選択的に空胞を持つ変性筋線維に封入体状に沈着していた[4]。

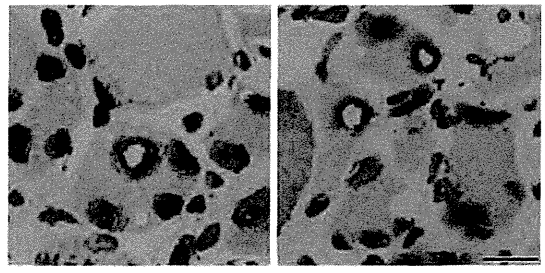

図　封入体筋炎筋組織におけるヒストンH1の免疫組織化学染色

核とともに空胞周囲に陽性反応が認められる。Bar＝20 μm

核マーカーとの二重染色ではどちらの封入体も核周囲にみられ，一部は核に陥凹を作っていた。CDK5とERK1/2は筋分化を促進する酵素であり，分化の際には細胞質から核に移行する。上記の結果は，疾患筋細胞では分化の段階において核で働くべき酵素が核内に移行できない状態であることを示すものと推定された。CDK5，ERK1/2の核輸送障害についても封入体筋炎における細胞核障害の一型と捉えることが可能である。

*

封入体筋炎の異常筋線維ではDNA二本鎖切断反応が亢進し，核崩壊，核輸送障害が示唆される。その根本原因を明らかにすることができれば，本疾患における筋変性の進行を防ぐ治療へとつながると思われる。

文　献

1) Nakano S, Kusaka H：Idiopathic Inflammatory Myopathies-Recent Developments, Gran JT (ed), pp143-162, InTech, Croatia, 2011
2) Nakano S et al：*Neuromuscul Disord* **18**：27-33, 2008
3) Konishi A et al：*Cell* **114**：673-688, 2003
4) Nishii M et al：*Neuromuscul Disord* **21**：345-352, 2011
5) Nakano S et al：*Neurology* **56**：87-93, 2001

Available online at www.sciencedirect.com

SciVerse ScienceDirect

Neuromuscular Disorders 22 (2012) 747–754

www.elsevier.com/locate/nmd

Case study

Inclusion body myositis coexisting with hypertrophic cardiomyopathy: An autopsy study

Yukie Inamori [a], Itsuro Higuchi [a,*], Teruhiko Inoue [b], Yusuke Sakiyama [a], Akihiro Hashiguchi [a], Keiko Higashi [a], Tadafumi Shiraishi [a], Ryuichi Okubo [a], Kimiyoshi Arimura [c], Yoshio Mitsuyama [b], Hiroshi Takashima [a]

[a] *Department of Neurology and Geriatrics, Kagoshima University Graduate School of Medical and Dental Sciences, Kagoshima, Japan*
[b] *Psychogeriatric Center, Daigo Hospital, Miyazaki, Japan*
[c] *Division of Neurology, Okatsu Hospital, Kagoshima, Japan*

Received 24 January 2012; received in revised form 16 March 2012; accepted 28 March 2012

Abstract

Inclusion body myositis is an inflammatory myopathy characterized pathologically by rimmed vacuoles and the accumulation of amyloid-related proteins. Autopsy studies in these patients, including histochemical examinations of multiple skeletal muscles, have not yet been published. In this paper, we describe the autopsy findings of a patient with inclusion body myositis and hypertrophic cardiomyopathy. A 69-year-old man, who was a human T lymphotropic virus type 1 carrier, exhibited slowly progressive muscle weakness and atrophy, predominantly affecting the scapular, quadriceps femoris, and forearm flexor muscles. His disease course was more rapidly progressive than that typically observed; the patient died suddenly of arrhythmia 5 years after diagnosis. Autopsy findings revealed that multiple muscles, including the respiratory muscles, were involved. Longitudinal studies revealed an increased frequency of rimmed vacuoles and p62/sequestosome 1- and/or TAR DNA-binding protein 43-positive deposits in autopsied muscles, although the amount of inflammatory infiltrate appeared to be decreased. We speculated that muscle degeneration may be more closely involved in disease progression compared with autoimmunity. Genetic analysis revealed a myosin binding protein C3 mutation, which is reportedly responsible for familial hypertrophic cardiomyopathy. This mutation and human T lymphotropic virus type 1 infection may have affected the skeletal muscles of this patient.

Keywords: Inclusion body myositis; Hypertrophic cardiomyopathy; Myosin binding protein C3 gene; Autopsy; Human T lymphotropic virus type 1

1. Introduction

Inclusion body myositis (IBM) is an inflammatory myopathy that clinically manifests as slowly progressive proximal and distal muscle weakness and most prominently affects the quadriceps, forearm flexors, and pharyngeal muscles. The etiology of IBM is unknown, and no successful treatment has been reported till date. In addition to inflammatory changes, IBM is pathologically characterized by the presence of rimmed vacuoles and the accumulation of amyloid-related proteins [1–4]. Phenotypic similarities between the muscle fibers of patients with IBM and the brains of patients with Alzheimer's disease have been reported [5–7]. Although IBM is generally sporadic, a few familial cases have been reported [8–13]. The involvement of genetic susceptibility factors in IBM has also been reported [9,14]. To the best of our knowledge, autopsy studies, including histochemical examinations of multiple skeletal muscles and the brain of IBM patients, have not yet been published.

* Corresponding author. Address: Department of Neurology and Geriatrics, Kagoshima University Graduate School of Medical and Dental Sciences, 8-35-1 Sakuragaoka, Kagoshima City, Kagoshima 890-8520, Japan. Tel.: +81 99 275 5332; fax: +81 99 265 7164.
E-mail address: ihiguchi@m2.kufm.kagoshima-u.ac.jp (I. Higuchi).

0960-8966/$ - see front matter © 2012 Elsevier B.V. All rights reserved.
http://dx.doi.org/10.1016/j.nmd.2012.03.011